

Binding Energies and Scattering Observables in the ${}^4\text{He}_3$ Atomic System*

A. K. Motovilov[†], W. Sandhas

Physikalisches Institut der Universität Bonn, Endenicher Allee 11-13, D-53115 Bonn, Germany

S. A. Sofianos

Physics Department, University of South Africa, P.O.Box 392, Pretoria 0003, South Africa

E. A. Kolganova

Joint Institute for Nuclear Research, Dubna, 141980, Russia

(November 8, 1999)

The ${}^4\text{He}_3$ bound states and the scattering of a ${}^4\text{He}$ atom off a ${}^4\text{He}$ dimer at ultra-low energies are investigated using a hard-core version of the Faddeev differential equations. Various realistic ${}^4\text{He}$ - ${}^4\text{He}$ interactions were employed, among them the LM2M2 potential by Aziz and Slaman and the recent TTY potential by Tang, Toennies and Yiu. The ground state and the excited (Efimov) state obtained are compared with other results. The scattering lengths and the atom-diatom phase shifts were calculated for center of mass energies up to 2.45 mK. It was found that the LM2M2 and TTY potentials, although of quite different structure, give practically the same bound-state and scattering results.

PACS numbers: 02.60.Nm, 21.45.+v, 34.40.-m, 36.40.+d

I. INTRODUCTION

Small ${}^4\text{He}$ clusters (in particular dimers and trimers) are of fundamental interest in various fields of physical chemistry and molecular physics. Studies of these clusters represent an important step towards understanding the properties of helium liquid drops, super-fluidity in ${}^4\text{He}$ films, the Bose-Einstein condensation *etc.* (see, for instance, Refs. [1–4]). Besides, the helium trimer is probably a unique molecular system where a direct manifestation of the Efimov effect [5] can be observed since the binding energy ϵ_d of the ${}^4\text{He}$ dimer is extremely small.

The ${}^4\text{He}$ trimer belongs to the three-body systems whose theoretical treatment is quite difficult, first, due to its Efimov nature and, second, because of the hard-core properties of the inter-atomic He–He interaction [6–9]. At the same time the problem of three helium atoms can be considered as an example of an ideal three-body quantum problem since ${}^4\text{He}$ atoms are identical neutral bosons and, thus, their handling is not complicated by spin, isospin, or Coulomb considerations.

There is a great number of experimental and theoretical studies of ${}^4\text{He}$ clusters. However, most of the theoretical investigations consist merely in computing the ground-state energy and are based on variational methods [10–15], on Hyperspherical Harmonics expansion methods in configuration space [16,17], and on integral equations in momentum space [18,19]. We further note that the results of Ref. [20] were based on a direct solution of the two-dimensional Faddeev differential equations in configuration space, while recently binding-energy results were obtained by using the three-dimensional Faddeev differential equations in the total-angular-momentum representation [21]. A qualitative treatment of the ${}^4\text{He}_3$ system in framework of an effective field theory is presented in Ref. [22].

In Refs. [15,16,19,23] it was pointed out that the excited state of the ${}^4\text{He}$ trimer is an Efimov state [5]. In these works the HFDHE2 [6], HFD-B [7], and LM2M2 [8] versions of the ${}^4\text{He}$ - ${}^4\text{He}$ potentials

*LANL E-print physics/9910016

[†]On leave of absence from the Joint Institute for Nuclear Research, Dubna, 141980, Russia

by Aziz and co-workers were employed. The essential property of this state is that it disappears when the inter-atomic potential is increased by a factor $\lambda \sim 1.2$. And vice versa, when λ slightly decreases (no more than 2%), a second excited state appears in the trimer [16,19]. It is just such a non-standard behavior of the excited-state energies which points at their Efimov nature. Another proof of such a nature of the excited state of the trimer, based on a scaling consideration, is discussed in [24]. The resonance mechanism of formation and disappearance of the Efimov levels in the ${}^4\text{He}_3$ system has been studied in Refs. [25,26].

The general atom-diatom collision problem has been addressed by various authors, and we refer the interested reader to the review articles [27] and [28]. The collision dynamics at thermal energies of the $\text{H}+\text{H}_2$ system and the existence of resonances were discussed in [29] using the Faddeev integral equations in momentum space. Finally, the problem of existence of ${}^4\text{He}$ n -mers and their relation to the Bose-Einstein condensation in HeII was discussed in Refs. [30,31]. From the experimental studies we mention those of Refs. [32–37] where molecular clusters, consisting of a small number of noble gas atoms, were investigated.

In contrast to the bulk of theoretical investigations devoted to the binding energies of the ${}^4\text{He}$ trimer, scattering processes found comparatively little attention. In Ref. [18] the characteristics of the $\text{He}-\text{He}_2$ scattering at zero energy were studied, while the recombination rate of the reaction $(1+1+1 \rightarrow 2+1)$ was estimated in [38]. Recently, the phase shifts of the $\text{He}-\text{He}_2$ elastic scattering and breakup amplitudes at ultra-low energies have also been calculated [23,39,40].

The difficulty in computing excited states and scattering observables in the ${}^4\text{He}_3$ system is mainly due to two reasons. First, the low energy ϵ_d of the dimer makes it necessary to consider very large domains in configuration space with a characteristic size of hundreds of Ångströms. Second, the strong repulsion of the $\text{He}-\text{He}$ interaction at short distances produces large numerical errors. In the present paper, which is an extension of our studies for ${}^4\text{He}_3$ [23,25,26,39,40], we employed the mathematically rigorous three-body Boundary Condition Model (BCM) of Refs. [41,42] to the above-mentioned problems.

As compared to [23,25,26,39,40] we employ, in the present work, the refined $\text{He}-\text{He}$ interatomic potentials LM2M2 by Aziz and Slaman [8], and TTY by Tang, Toennies, and Yiu [9]. Our numerical methods have been substantially improved, and this allowed us to use considerably larger grids achieving, thus, a better accuracy. Furthermore, due to much better computing facilities more partial waves could be taken into account.

This paper is organized as follows. In Sec. II we review the three-body bound and scattering state formalism for hard-core interactions. In Sec. III we describe its application to the system of three ${}^4\text{He}$ atoms and present our numerical results. Our conclusions are summarized in Sec. IV. Finally in the Appendix we give details of the potentials used.

II. FORMALISM

A detailed analysis of the general boundary-value problem, the derivation of the asymptotic boundary conditions for scattering states and other boundary-value formulations, can be found in Refs. [43,44]. In this work we employ a hard-core version of the BCM [42,45] developed in [41,46] (for details see Ref. [23]). Therefore, in what follows we shall only outline the formalism and present its main characteristics.

In describing the three-body system we use the standard Jacobi coordinates $\mathbf{x}_\alpha, \mathbf{y}_\alpha$, $\alpha = 1, 2, 3$, expressed in terms of the position vectors of the particles \mathbf{r}_i and their masses m_i ,

$$\mathbf{x}_\alpha = \left[\frac{2m_\beta m_\gamma}{m_\beta + m_\gamma} \right]^{1/2} (\mathbf{r}_\beta - \mathbf{r}_\gamma)$$

$$\mathbf{y}_\alpha = \left[\frac{2m_\alpha(m_\beta + m_\gamma)}{m_\alpha + m_\beta + m_\gamma} \right]^{1/2} \left(\mathbf{r}_\alpha - \frac{m_\beta \mathbf{r}_\beta + m_\gamma \mathbf{r}_\gamma}{m_\beta + m_\gamma} \right)$$

where (α, β, γ) stands for a cyclic permutation of the indices $(1, 2, 3)$.

In the so-called hard-core potential model one requires that the wave function vanishes when the particles approach each other at a certain distance $r = c$. This requirement is equivalent to the introduction of an infinitely strong repulsion between the particles at distances $r \leq c$. Such a replacement of the repulsive short-range part of the potential by a hard-core interaction turns out to be a very efficient way to suppress inaccuracies at short distances. One can then show that the Faddeev components satisfy the following system of differential equations

$$\begin{cases} (-\Delta_X + V_\alpha - E)\Phi_\alpha(X) = -V_\alpha \sum_{\beta \neq \alpha} \Phi_\beta(X), & |\mathbf{x}_\alpha| > c_\alpha, \\ (-\Delta_X - E)\Phi_\alpha(X) = 0, & |\mathbf{x}_\alpha| < c_\alpha. \end{cases} \quad (1)$$

where $X \equiv (\mathbf{x}_\alpha, \mathbf{y}_\alpha)$, $\alpha = 1, 2, 3$ and c_α is the hard-core radius in the channel α .

Outside the core the components Φ_α still provide the total wave function Ψ ,

$$\Psi(X) = \sum_{\beta=1}^3 \Phi_\beta(X),$$

while in the interior region we have

$$\sum_{\beta=1}^3 \Phi_\beta(X) \equiv 0.$$

In practice, one can replace the latter strong condition by a more weak one [41,46],

$$\sum_{\beta=1}^3 \Phi_\beta(X) \Big|_{|\mathbf{x}_\alpha|=c_\alpha} = 0, \quad \alpha = 1, 2, 3, \quad (2)$$

which requires the sum of $\Phi_\alpha(X)$ to be zero only at the radius c_α .

The numerical advantage of our approach is already obvious from the structure of Eqs. (1). When a potential with a strong repulsive core is replaced by the hard-core model, one approximates inside the core domains only the Laplacian Δ_X instead of the sum of the Laplacian and the huge repulsive term. In this way a much better numerical approximation can be achieved.

In the present investigation we apply the formalism to the ^4He three-atomic system with total angular momentum $L = 0$. The partial-wave version of the equations (1) for a system of three identical bosons with $L = 0$ reads [47,48]

$$\left[-\frac{\partial^2}{\partial x^2} - \frac{\partial^2}{\partial y^2} + l(l+1) \left(\frac{1}{x^2} + \frac{1}{y^2} \right) - E \right] \Phi_l(x, y) = \begin{cases} -V(x)\Psi_l(x, y), & x > c \\ 0, & x < c. \end{cases} \quad (3)$$

Here, x, y are the absolute values of the Jacobi variables and c is the core size which is the same for all three two-body subsystems. The angular momentum l corresponds to a dimer subsystem and a complementary atom. For a three-boson system in an S -state l can only be even, $l = 0, 2, 4, \dots$. The

potential $V(x)$ is assumed to be central and the same for all partial waves l . The function $\Psi_l(x, y)$ is related to the partial-wave Faddeev components $\Phi_l(x, y)$ by

$$\Psi_l(x, y) = \Phi_l(x, y) + \sum_{l'} \int_{-1}^{+1} d\eta h_{ll'}(x, y, \eta) \Phi_{l'}(x', y') \quad (4)$$

where

$$x' = \sqrt{\frac{1}{4}x^2 + \frac{3}{4}y^2 - \frac{\sqrt{3}}{2}xy\eta}, \quad y' = \sqrt{\frac{3}{4}x^2 + \frac{1}{4}y^2 + \frac{\sqrt{3}}{2}xy\eta},$$

with $\eta = \hat{\mathbf{x}} \cdot \hat{\mathbf{y}}$. Expressions for the kernels $h_{ll'}$ can be found in [23,47,48]. It should be noted that these kernels depend only on the hyperangles

$$\theta = \arctan \frac{y}{x} \quad \text{and} \quad \theta' = \arctan \frac{y'}{x'}$$

and not on the hyperradius

$$\rho = \sqrt{x^2 + y^2} = \sqrt{x'^2 + y'^2}.$$

The functions $\Phi_l(x, y)$ satisfy the boundary conditions

$$\Phi_l(x, y)|_{x=0} = \Phi_l(x, y)|_{y=0} = 0. \quad (5)$$

The partial-wave version of the hard-core boundary condition (2) reads

$$\Phi_l(c, y) + \sum_{l'} \int_{-1}^{+1} d\eta h_{ll'}(c, y, \eta) \Phi_{l'}(x', y') = 0 \quad (6)$$

requiring the wave function $\Psi_l(x, y)$ to be zero at the core boundary $x = c$. Furthermore, one can show that, in general, the condition (6), like the condition (2), causes also the wave functions (4) to vanish inside the core domains. For the bound-state problem one requires that the functions $\Phi_l(x, y)$ are square integrable in the quadrant $x \geq 0, y \geq 0$.

The asymptotic condition for the helium trimer scattering states reads

$$\begin{aligned} \Phi_l(x, y) = & \delta_{l0} \psi_d(x) \exp(i\sqrt{E_t - \epsilon_d}y) [a_0 + o(y^{-1/2})] \\ & + \frac{\exp(i\sqrt{E_t}\rho)}{\sqrt{\rho}} [A_l(\theta) + o(\rho^{-1/2})] \end{aligned} \quad (7)$$

as $\rho \rightarrow \infty$ and/or $y \rightarrow \infty$. Here we use the fact that the helium dimer bound state exists only for $l = 0$. ϵ_d stands for the dimer energy while $\psi_d(x)$ denotes the dimer wave function which is assumed to be zero within the core, i. e., $\psi_d(x) \equiv 0$ for $x \leq c$.

The coefficients a_0 and $A_l(\theta)$ describe the contributions of the $(2+1)$ and $(1+1+1)$ channels to Φ_l , respectively. Both the trimer binding energy E_t and the difference $E_t - \epsilon_d$ in (7) are negative which means that for any θ the function $\Phi_l(x, y)$ decreases exponentially as $\rho \rightarrow \infty$.

The asymptotic boundary condition for the partial-wave Faddeev components of the $(2+1 \rightarrow 2+1; 1+1+1)$ scattering wave function reads, as $\rho \rightarrow \infty$ and/or $y \rightarrow \infty$,

$$\begin{aligned} \Phi_l(x, y; p) = & \delta_{l0} \psi_d(x) \{ \sin(py) + \exp(ipy) [a_0(p) + o(y^{-1/2})] \} \\ & + \frac{\exp(i\sqrt{E}\rho)}{\sqrt{\rho}} [A_l(E, \theta) + o(\rho^{-1/2})] \end{aligned} \quad (8)$$

where p is the relative momentum conjugate to the variable y , E is the scattering energy given by $E = \epsilon_d + p^2$, and $a_0(p)$ is the elastic scattering amplitude. The functions $A_l(E, \theta)$ provide us for $E > 0$ with the corresponding partial-wave breakup amplitudes.

The helium-atom helium-dimer scattering length ℓ_{sc} is given by

$$\ell_{\text{sc}} = -\frac{\sqrt{3}}{2} \lim_{p \rightarrow 0} \frac{a_0(p)}{p}$$

while the S -state elastic scattering phase shifts $\delta_0(p)$ are given by

$$\delta_0(p) = \frac{1}{2} \text{Im} \ln S_0(p) \quad (9)$$

where $S_0(p) = 1 + 2ia_0(p)$ is the $(2 + 1 \rightarrow 2 + 1)$ partial-wave component of the scattering matrix.

III. RESULTS

We employed the Faddeev equations (3) and the hard-core boundary condition (6) to calculate the binding energies of the helium trimer and the ultra-low energy phase shifts of the helium atom scattered off the helium diatomic molecule. As He-He interaction we used three versions of the semi-empirical potentials of Aziz and collaborators, namely HFDHE2 [6], HFD-B [7], and the newer version LM2M2 [8]. Further, we employed the latest theoretical He-He potential TTY of Tang et al. [9]. These potentials are given in the Appendix. In our calculations we used the value $\hbar^2/m = 12.12 \text{ K \AA}^2$. All the potentials considered produce a weakly bound dimer state. The energy ϵ_d of this state together with the He-He atomic scattering length $\ell_{\text{sc}}^{(2)}$ are given in Table I. It is interesting to note that the latest potentials LM2M2 and TTY give practically the same scattering length ℓ_{sc} and dimer energy ϵ_d .

A detailed description of our numerical method has been given in Ref. [23]. Therefore, we outline here only the main steps of the computational scheme employed to solve the boundary-value problems (3), (5), (6) and (7) or (8). First, we note that the grid for the finite-difference approximation of the polar coordinates ρ and θ is chosen such that the points of intersection of the arcs $\rho = \rho_i$, $i = 1, 2, \dots, N_\rho$ and the rays $\theta = \theta_j$, $j = 1, 2, \dots, N_\theta$ with the core boundary $x = c$ constitute the knots. The value of c was fixed to be such that any further decrease of it did not appreciably influence the dimer binding energy ϵ_d and the energy of the trimer ground state $E_t^{(0)}$. In our previous work [23,39,40] c was chosen as 0.7 \AA . In the present work, however, we choose $c = 1.0 \text{ \AA}$. This value of c provides a dimer bound state ϵ_d which is stable within six figures and a trimer ground-state energy $E_t^{(0)}$ stable within three figures. The ρ_i are chosen according to the formulas

$$\begin{aligned} \rho_i &= \frac{i}{N_c^{(\rho)} + 1} c, & i = 1, 2, \dots, N_c^{(\rho)}, \\ \rho_{i+N_c^{(\rho)}} &= \sqrt{c^2 + y_i^2}, & i = 1, 2, \dots, N_\rho - N_c^{(\rho)}, \end{aligned}$$

where $N_c^{(\rho)}$ stands for the number of arcs inside the domain $\rho < c$ and

$$y_i = f(\tau_i) \sqrt{\rho_{N_\rho}^2 - c^2}, \quad \tau_i = \frac{i}{N_\rho - N_c^{(\rho)}}.$$

The nonlinear monotonously increasing function $f(\tau)$, $0 \leq \tau \leq 1$, satisfying the conditions $f(0) = 0$ and $f(1) = 1$, is chosen according to

$$f(\tau) = \begin{cases} \alpha_0 \tau & , \tau \in [0, \tau_0] \\ \alpha_1 \tau + \tau^\nu & , \tau \in (\tau_0, 1] \end{cases} .$$

The values of α_0 , $\alpha_0 \geq 0$, and α_1 , $\alpha_1 \geq 0$, are determined via τ_0 and ν from the continuity condition for $f(\tau)$ and its derivative at the point τ_0 . In the present investigation we took values of τ_0 within 0.15 and 0.2. The value of the power ν depends on the cutoff radius $\rho_{\max} = \rho_{N_\rho} = 200\text{--}1000 \text{ \AA}$, its range being within 3.4 and 4 in the present calculations.

The knots θ_j at $j = 1, 2, \dots, N_\rho - N_c^{(\rho)}$ are taken according to $\theta_j = \arctan(y_j/c)$ with the remaining knots θ_j , $j = N_\rho - N_c^{(\rho)} + 1, \dots, N_\theta$, being chosen equidistantly. Such a choice is required by the need of having a higher density of points in the domain where the functions $\Phi_l(x, y; z)$ change most rapidly, i. e., for small values of ρ and/or x . In this work, we used grids of the dimension $N_\theta = N_\rho = 500\text{--}800$ while the above number $N_c^{(\rho)}$ and the number $N_\theta - (N_\rho - N_c^{(\rho)})$ of knots in θ lying in the last arc inside the core domain was chosen equal to 2–5.

Since we consider identical bosons only the components Φ_l corresponding to even l differ from zero. Thus, the number of equations to be solved is $N_e = l_{\max}/2 + 1$ where l_{\max} is the maximal even partial wave. The finite-difference approximation of the N_e equations (3) reduces the problem to a system of $N_e N_\theta N_\rho$ linear algebraic equations. The finite-difference equations corresponding to the arc $i = N_\rho$ include initially the values of the unknown functions $\Phi_l(x, y; z)$ from the arc $i = N_\rho + 1$. To eliminate them, we express these values through the values of $\Phi_l(x, y; z)$ on the arcs $i = N_\rho$ and $i = N_\rho - 1$ by using the asymptotic formulas (7) or (8) in the manner described in the final part of Appendix A of Ref. [23]. In [23], however, this approach was used for computing the binding energies only, while in the present work this method is extended also to the scattering problem. The matrix of the resulting system of equations has a block three-diagonal form. Every block has the dimension $N_e N_\theta \times N_e N_\theta$ and consists of the coefficients standing at unknown values of the Faddeev components in the grid knots belonging to a certain arc $\rho = \rho_i$. The main diagonal of the matrix consists of N_ρ such blocks.

In this work we solve the block three-diagonal algebraic system on the basis of the matrix sweep method [49]. The use of this method makes it possible to avoid writing the matrix on the hard drive of the computer. Besides, the matrix sweep method reduces the computer time required by almost one order of magnitude as compared to [23,39,40].

Our results for the trimer ground-state energy $E_t^{(0)}$, as well as the results obtained by other authors, are presented in Table II. It should be noted that most of the contribution to the ground-state energy stems from the $l = 0$ and $l = 2$ partial-wave components, the latter being slightly more than 30 %, and is approximately the same for all potentials used. The contribution from the $l = 4$ partial wave is of the order of 3–4 % (cf. [20]).

It is well known that the excited state of the ^4He trimer is an Efimov state [16,19,23,25,26]. The results obtained for its energy $E_t^{(1)}$, as well as the results found in the literature, are presented in Table III. To illustrate the convergence of our results we show in Table IV the dependence of $E_t^{(1)}$ on the grid parameters using the TTY potential. It is seen that the $l = 0$ partial-wave component contributes about 71 % to the excited-state binding energy. The contribution to $E_t^{(1)}$ from the $l = 2$ component is about 25–26 % and from $l = 4$ within 3–4 %. These values are similar to the ones for the ground state.

Besides the binding-energy calculations, we also performed calculations for a helium atom scattered off a helium dimer for $L = 0$. For this we used the asymptotic boundary conditions (8). The

scattering lengths of the collision of the He atom on the He dimer obtained for the HFD-B, LM2M2 and TTY potentials are presented in Table V. As compared to [23] the present calculation is essentially improved (the result $\ell_{sc} = 145 \pm 5 \text{ \AA}$ for HFD-B with $l_{\max} = 2$ was obtained in [23] with a much smaller grid). Within the accuracy of our calculations, the scattering lengths provided by the LM2M2 and TTY potentials, like the energies of the excited state, are exactly the same. This is of no surprise since the two potentials produce practically the same two-body binding energies and scattering lengths.

The phase-shift results obtained for the HFD-B, LM2M2 and TTY potentials are given in Tables VI, VII, and VIII. For the HFD-B and TTY potentials they are plotted in Fig. 1. Note that for the phase shifts we use the normalization required by the Levinson theorem [50], $\delta_L(0) - \delta_L(\infty) = n\pi$, where n is the number of the trimer bound states.

Incident energies below and above the breakup threshold were considered, i. e., for the $(2 + 1 \rightarrow 2 + 1)$ and $(2 + 1 \rightarrow 1 + 1 + 1)$ processes. It was found that after transformation to the laboratory system the phases $\delta_0^{(l_{\max})}$ for the potentials HFD-B, LM2M2 and TTY for different values of l_{\max} are practically the same, especially those for LM2M2 and TTY. The difference between the phase shifts $\delta_0^{(2)}$ and $\delta_0^{(4)}$ is only about 0.5 %.

It is interesting to compare the values obtained for the He–He₂ scattering lengths ℓ_{sc} with the corresponding inverse wave numbers \varkappa^{-1} for the trimer excited-state energies. The values of \varkappa^{-1} where $\varkappa = 2\sqrt{(\epsilon_d - E_t^{(1)})/3}$, with both the $E_t^{(1)}$ and ϵ_d being given in \AA^{-2} , are also presented in Table V. It is seen that these numbers are about 1.3–1.7 times smaller than the respective ⁴He-atom ⁴He-dimer scattering lengths. The situation differs completely from the ⁴He two-atomic scattering problem, where the inverse wave numbers $(\varkappa^{(2)})^{-1} = |\epsilon_d|^{-1/2}$ are in a rather good agreement with the ⁴He–⁴He scattering lengths (see Table I). Such significant differences between ℓ_{sc} and \varkappa^{-1} in the case of the ⁴He three-atomic system can be attributed to the Efimov nature of the excited state of the trimer, which implies that the effective range r_0 for the interaction between the ⁴He atom and the ⁴He dimer is very large as compared to the ⁴He diatomic problem.

IV. CONCLUSIONS

In this paper we employed a hard-core variant of the Boundary Condition Model which, unlike some competing methods, is exact and ideally suited for three-body calculations with two-body interactions characterized by a highly repulsive core. The method is relevant not only for bound states but also for scattering processes. There is, however, a price to be paid for the exact treatment of the system. Higher partial waves, beyond $l_{\max} = 4$, were hard to be incorporated within the computing facilities at our disposal.

The results for the ground-state energy of the ⁴He trimer obtained for all four ⁴He–⁴He potentials considered compare favorably with alternative results in the literature. Furthermore, the treatment of the excited state, interpreted as an Efimov state, clearly demonstrates the reliability of our method in three-body bound state calculations with hard-core potentials. In addition to the binding energy, the formalism has been successfully used to calculate scattering lengths and ultra-low-energy phase shifts of the ⁴He atom scattered off the ⁴He dimer.

In general the hard-core inter-atomic potential together with other characteristics of the system, makes calculations extremely tedious and numerically unstable. This is not the case in our formalism where the hard core is taken into account from the very beginning in a mathematically rigorous way. Thus, the formalism paves the way to study various ultra-cold three-atom systems, and to calculate important quantities as cross-sections, recombination rates, *etc.*

ACKNOWLEDGMENTS

The authors are grateful to Prof. V. B. Belyaev and Prof. H. Toki for help and assistance in performing the calculations at the supercomputer of the Research Center for Nuclear Physics of the Osaka University, Japan. One of the authors (W. S.) would like to thank J. P. Toennies for very interesting discussions stimulating this investigation. Financial support by the Deutsche Forschungsgemeinschaft, the Russian Foundation for Basic Research, and the National Research Foundation of South Africa, is gratefully acknowledged.

APPENDIX: THE POTENTIALS USED

The general structure of the realistic semi-empirical potentials HFDHE2 [6] and HFD-B [7] developed by Aziz *et al.* is

$$V(x) = \varepsilon V_b(\zeta) \tag{A1}$$

where $\zeta = x/r_m$ and the term $V_b(\zeta)$ reads

$$V_b(\zeta) = A \exp(-\alpha\zeta + \beta\zeta^2) - \left[\frac{C_6}{\zeta^6} + \frac{C_8}{\zeta^8} + \frac{C_{10}}{\zeta^{10}} \right] F(\zeta),$$

x is expressed in the same length units as r_m (\AA in the present case). The function $F(\zeta)$ is given by

$$F(\zeta) = \begin{cases} \exp[-(D/\zeta - 1)]^2, & \text{if } \zeta \leq D \\ 1, & \text{if } \zeta > D. \end{cases}$$

In addition to the term $V_b(\zeta)$ the LM2M2 potential [8] contains a term $V_a(\zeta)$,

$$V(r) = \varepsilon \{V_b(\zeta) + V_a(\zeta)\}, \tag{A2}$$

where

$$V_a(\zeta) = \begin{cases} A_a \left\{ \sin \left[\frac{2\pi(\zeta - \zeta_1)}{\zeta_2 - \zeta_1} - \frac{\pi}{2} \right] + 1 \right\}, & \zeta_1 \leq \zeta \leq \zeta_2 \\ 0, & \zeta \notin [\zeta_1, \zeta_2]. \end{cases}$$

The parameters for the HFDHE2, HFD-B and LM2M2 potentials are given in Table IX.

The form of the theoretical He-He potential TTY is taken from [9]. This potential reads

$$V(x) = A [V_{\text{ex}}(x) + V_{\text{disp}}(x)]$$

where x stands for the distance between the ^4He atoms given in atomic length units. (Following [9] in converting the length units we used $1 \text{ a.u.} = 0.52917 \text{ \AA}$.) The function V_{ex} has the form

$$V_{\text{ex}}(x) = D x^p \exp(-2\beta x)$$

with $p = \frac{7}{2\beta} - 1$, while the function V_{disp} reads

$$V_{\text{disp}}(x) = - \sum_{n=3}^N C_{2n} f_{2n}(x) x^{-2n}.$$

The coefficients C_{2n} are calculated via the recurrency relation

$$C_{2n} = \left(\frac{C_{2n-2}}{C_{2n-4}} \right)^3 C_{2n-6},$$

and the functions f_{2n} are given by

$$f_{2n}(x) = 1 - \exp(-bx) \sum_{k=0}^{2n} \frac{(bx)^k}{k!}$$

where

$$b(x) = 2\beta - \left[\frac{7}{2\beta} - 1 \right] \frac{1}{x}.$$

The parameters of the TTY potential are given in Table X.

- [1] J. P. Toennies and K. Winkelmann, *J. Chem. Phys.* **66**, 3965 (1977).
- [2] M. V. Rama Krishna and K. B. Whaley, *Phys. Rev. Lett.* **64**, 1126 (1990).
- [3] K. K. Lehman and G. Scoles, *Science* **279**, 2065 (1998).
- [4] S. Grebenev, J. P. Toennies, and A. F. Vilesov, *Science* **279**, 2083 (1998).
- [5] V. Efimov, *Nucl. Phys. A* **210**, 157 (1973).
- [6] R. A. Aziz, V. P. S. Nain, J. S. Carley, W. L. Taylor, and G. T. McConville, *J. Chem. Phys.* **79**, 4330 (1979).
- [7] R. A. Aziz, F. R. W. McCourt, and C. C. K. Wong, *Mol. Phys.* **61**, 1487 (1987).
- [8] R. A. Aziz and M. J. Slaman, *J. Chem. Phys.* **94**, 8047 (1991).
- [9] K. T. Tang, J. P. Toennies, and C. L. Yiu, *Phys. Rev. Lett.* **74**, 1546 (1995).
- [10] S. W. Rick, D. L. Lynch, and J. D. Doll, *J. Chem. Phys.* **95**, 3506 (1991).
- [11] V. R. Pandharipande, J. G. Zabolitzky, S. C. Pieper, R. B. Wiringa, and U. Helmbrecht, *Phys. Rev. Lett.*, **50**, 1676 (1983).
- [12] R. N. Barnett and K. B. Whaley, *Phys. Rev. A* **47**, 4082 (1993).
- [13] M. Lewerenz, *J. Chem. Phys.* **106**, 4596 (1997).
- [14] R. Guardiola, M. Portesi, and J. Navarro, LANL E-print physics/9904037.
- [15] T. González-Lezana, J. Rubayo-Soneira, S. Miret-Artés, F. A. Gianturco, G. Delgado-Barrio, and P. Villareal, *Phys. Rev. Lett.* **82**, 1648 (1999).
- [16] B. D. Esry, C. D. Lin, and C. H. Greene, *Phys. Rev. A* **54**, 394 (1996).
- [17] E. Nielsen, D. V. Fedorov, and A. S. Jensen, *J. Phys. B* **31**, 4085 (1998) (LANL E-print physics/9806020).
- [18] S. Nakaichi-Maeda and T. K. Lim, *Phys. Rev. A* **28**, 692 (1983).
- [19] Th. Corneliuss and W. Glöckle, *J. Chem. Phys.* **85**, 3906 (1986).
- [20] J. Carbonell, C. Gignoux, and S. P. Merkuriev, *Few-Body Systems* **15**, 15 (1993).
- [21] V. Roudnev and S. Yakovlev, LANL E-print physics/9910030.
- [22] P. F. Bedaque, H.-W. Hammer, and U. van Kolck, *Nucl. Phys. A* **646**, 444 (1999) (LANL E-print nucl-th/9811046).
- [23] E. A. Kolganova, A. K. Motovilov, and S. A. Sofianos, *J. Phys. B.* **31**, 1279 (1998) (LANL E-print physics/9612012).
- [24] T. Frederico, L. Tomio, A. Delfino, and A. E. A. Amorim, *Phys. Rev. A* **60**, R9 (1999).
- [25] A. K. Motovilov and E. A. Kolganova, *Few-Body Systems Suppl.* **10**, 75 (1999) (LANL E-print physics/9810006).
- [26] E. A. Kolganova and A. K. Motovilov, *Phys. Atom. Nucl.* **62** No. 7, 1179 (1999) (LANL E-print physics/9808027).
- [27] D. A. Micha, *Nucl. Phys. A* **353**, 309 (1981).
- [28] A. Kuppermann, *Nucl. Phys. A* **353**, 287 (1981).
- [29] Z. C. Kuruoglu and D. A. Micha, *J. Chem. Phys.* **80**, 4262 (1980).
- [30] H. B. Ghassib and G. V. Chester, *J. Chem. Phys.* **82**, 585 (1984).
- [31] N. H. March, *J. Chem. Phys.* **82**, 587 (1984).
- [32] F. Luo, G. C. McBane, G. Kim, C. F. Giese, and W. R. Gentry, *J. Chem. Phys.* **98**, 3564 (1993).
- [33] F. Luo, C. F. Giese, and W. R. Gentry, *J. Chem. Phys.* **104**, 1151 (1996).
- [34] W. Schöllkopf and J. P. Toennies, *Science* **266**, 1345 (1994).
- [35] U. Buck and H. Meyer, *J. Chem. Phys.* **84**, 4854 (1986).

- [36] O. Echt, K. Sattler, and E. Recknagel, Phys. Rev. Lett. **47**, 1121 (1981).
- [37] W. Schöllkopf and J. P. Toennies, J. Chem. Phys. **104**, 1155 (1996).
- [38] P. O. Fedichev, M. W. Reynolds, and G. V. Shlyapnikov, Phys. Rev. Lett. **77**, 2921 (1996).
- [39] E. A. Kolganova, A. K. Motovilov and S. A. Sofianos, Phys. Rev. A. **56**, R1686 (1997) (LANL E-print physics/9802016).
- [40] A. K. Motovilov, S. A. Sofianos, and E. A. Kolganova, Chem. Phys. Lett. **275**, 168 (1997) (LANL E-print physics/9709037).
- [41] S. P. Merkuriev and A. K. Motovilov, Lett. Math. Phys. **7**, 497 (1983).
- [42] S. P. Merkuriev, A. K. Motovilov, and S. L. Yakovlev, Theor. Math. Phys. **94**, 306 (1993).
- [43] A. K. Motovilov, *Three-body quantum problem in the boundary-condition model* (PhD thesis (in Russian), Leningrad State University, Leningrad, 1984).
- [44] A. A. Kvitsinsky, Yu. A. Kuperin, S. P. Merkuriev, A. K. Motovilov, and S. L. Yakovlev, Sov. J. Part. Nucl. **17**, 113 (1986).
- [45] V. N. Efimov and H. Schulz, Sov. J. Part. Nucl. **7**, 349 (1976).
- [46] A. K. Motovilov, Vestnik Leningradskogo Universiteta, **22**, 76 (1983).
- [47] L. D. Faddeev and S. P. Merkuriev, *Quantum scattering theory for several particle systems* (Dordrecht: Kluwer Academic Publishers, 1993).
- [48] S. P. Merkuriev, C. Gignoux, and A. Laverne, Ann. Phys. (N.Y.) **99**, 30 (1976).
- [49] A. A. Samarsky: *Theory of difference schemes* (in Russian) (Nauka, Moscow, 1977).
- [50] N. Levinson, K. Dan. Vidensk. Selsk. Mat. Fys. Medd. **25**, 9 (1949).

TABLE I. Dimer energies ϵ_d , inverse wave lengths $1/\varkappa^{(2)}$, and ${}^4\text{He}-{}^4\text{He}$ scattering lengths $\ell_{\text{sc}}^{(2)}$ for the potentials used.

Potential	E_d (mK)	$1/\varkappa^{(2)}$ (Å)	$\ell_{\text{sc}}^{(2)}$ (Å)	Potential	E_d (mK)	$1/\varkappa^{(2)}$ (Å)	$\ell_{\text{sc}}^{(2)}$ (Å)
HFDHE2	-0.83012	120.83	124.65	LM2M2	1.30348	96.43	100.23
HFD-B	-1.68541	84.80	88.50	TTY	1.30962	96.20	100.01

TABLE II. Ground state energy $E_t^{(0)}$ results for the helium trimer. The (absolute) values of $E_t^{(0)}$ are given in K. The grid parameters used were: $N_\theta = N_\rho = 555$, $\tau_0 = 0.2$, $\nu = 3.6$, and $\rho_{\text{max}} = 250$ Å.

Potential	Faddeev equations						Variational methods					Adiabatic approaches	
	l_{max}	This work	[20]	[19]	[18]	[21]	[11]	[10]	[12]	[13]	[14]	[16]	[17]
HFDHE2	0	0.084 ^{a)}	0.0823		0.082	0.092							
	2	0.114 ^{a)}	0.1124	0.107	0.11								
	4	0.1167				0.1171	0.1173						
HFD-B	0	0.096 ^{a)}	0.0942	0.096									
	2	0.131 ^{a)}	0.1277	0.130									
	4	0.1325				0.1330	0.1193	0.133	0.131	0.129			
LM2M2	0	0.0891										0.106	
	2	0.1213											
	4	0.1259				0.1264							0.1252
TTY	0	0.0890											
	2	0.1212											
	4	0.1258				0.1264			0.126				

^{a)}Results from [23] for a grid with $N_\theta = N_\rho = 275$ and $\rho_{\text{max}} = 60$ Å.

TABLE III. Excited state energy $E_t^{(1)}$ results for the helium trimer. The (absolute) values of $E_t^{(1)}$ are given in mK. The grid parameters used were: $N_\theta = N_\rho = 805$, $\tau_0 = 0.2$, $\nu_0 = 3.6$, and $\rho_{\text{max}} = 300$ Å.

Potential	l_{max}	This work	[19]	[18]	[21]	[16]	[17]
HFDHE2	0	1.5 ^{a)}	1.46	1.46	1.04	1.517	
	2	1.7 ^{a)}	1.65	1.6			
	4	1.67				1.665	
HFD-B	0	2.5 ^{a)}	2.45				
	2	2.8 ^{a)}	2.71				
	4	2.74				2.734	
LM2M2	0	2.02				2.118	
	2	2.25					
	4	2.28				2.271	2.269
TTY	0	2.02					
	2	2.25					
	4	2.28				2.280	

^{a)}Results from [23] for a grid with $N_\theta = N_\rho = 252$ and $\rho_{\text{max}} = 250$ Å.

TABLE IV. Trimer excited-state energy $E_t^{(1)}$ (mK) obtained with the TTY potential for various grids.

l_{\max}	$N_\theta = N_\rho = 252$ $\rho_{\max} = 250 \text{ \AA}$	$N_\theta = N_\rho = 502$ $\rho_{\max} = 300 \text{ \AA}$	$N_\theta = N_\rho = 652$ $\rho_{\max} = 300 \text{ \AA}$	$N_\theta = N_\rho = 805$ $\rho_{\max} = 300 \text{ \AA}$	$N_\theta = N_\rho = 1005$ $\rho_{\max} = 300 \text{ \AA}$
0	-2.108	-2.039	-2.029	-2.024	-2.021
2	-2.348	-2.273	-2.258	-2.253	-2.248

 TABLE V. Estimations for ${}^4\text{He}$ atom- ${}^4\text{He}$ dimer scattering lengths ℓ_{sc} and inverse wave numbers \varkappa^{-1} corresponding to the excited-state energy $E_t^{(1)}$ for the HFD-B, LM2M2 and TTY potentials. The accuracy for the scattering lengths is within $\pm 5 \text{ \AA}$. The grid parameters used for the calculation of ℓ_{sc} are: $N_\theta = N_\rho = 502$, $\tau_0 = 0.18$, $\nu = 3.45$ and $\rho_{\max} = 460 \text{ \AA}$.

Potential	l_{\max}	ℓ_{sc} (Å)	\varkappa^{-1} (Å)	Potential	l_{\max}	ℓ_{sc} (Å)	\varkappa^{-1} (Å)
HFD-B	0	170 ^{a)} 168	109	LM2M2/TTY	0	168	113
	2	145 ^{a)} 138	94		2	134	98
	4	135	93		4	131	96

^{a)}Results from [23] for a grid with $N_\theta = N_\rho = 320$ and $\rho_{\max} = 400 \text{ \AA}$.

 TABLE VI. Phase shift $\delta_0^{(l_{\max})}$ results (in degrees) for the HFD-B potential for various c.m. energies E (in mK). The grid parameters used are: $N_\theta = N_\rho = 502$, $\tau_0 = 0.18$, $\nu = 3.45$, and $\rho_{\max} = 460 \text{ \AA}$.

E	$\delta_0^{(0)}$	$\delta_0^{(2)}$	$\delta_0^{(4)}$	E	$\delta_0^{(0)}$	$\delta_0^{(2)}$	$\delta_0^{(4)}$	E	$\delta_0^{(0)}$	$\delta_0^{(2)}$	$\delta_0^{(4)}$
-1.68541	359.9	359.9	359.9	-1.05	299.1	308.2	309.2	0.95	262.4	272.1	273.7
-1.68	352.6	353.9	354.1	-0.8	290.8	300.4	301.5	1.2	260.0	269.6	270.7
-1.65	341.7	345.0	345.4	-0.55	284.4	294.2	295.4	1.45	257.8	267.3	268.4
-1.60	330.8	337.7	338.2	-0.3	279.3	289.3	290.4	1.7	255.9	265.2	266.3
-1.55	326.9	332.8	333.5	-0.05	275.1	285.2	286.3	1.95	254.1	263.4	264.5
-1.50	322.4	329.0	329.8	0.2	271.4	281.3	282.5	2.2	252.5	261.7	262.7
-1.40	315.4	323.0	323.9	0.45	268.1	277.9	279.0	2.45	251.0	260.1	261.1
-1.30	309.9	318.1	319.1	0.7	265.1	274.8	276.0				

 TABLE VII. Phase shift $\delta_0^{(l_{\max})}$ results for the LM2M2 potential. The units and grid parameters used are the same as in Table VI.

E	$\delta_0^{(0)}$	$\delta_0^{(2)}$	E	$\delta_0^{(0)}$	$\delta_0^{(2)}$	E	$\delta_0^{(0)}$	$\delta_0^{(2)}$
-1.30348	359.8	359.9	-0.8	304.6	313.8	0.95	267.0	276.2
-1.3	354.1	355.3	-0.55	295.2	304.8	1.2	264.1	273.2
-1.25	337.9	342.3	-0.3	287.9	297.7	1.45	261.5	270.6
-1.20	330.5	336.3	-0.05	282.3	292.2	1.7	259.2	268.1
-1.15	325.2	332.0	0.2	277.7	287.4	1.95	257.1	266.0
-1.10	321.1	328.5	0.45	273.7	283.2	2.2	255.3	264.0
-1.05	317.6	325.5	0.7	270.1	279.5	2.45	253.6	262.3

TABLE VIII. Phase shift $\delta_0^{(l_{\max})}$ results for the TTY potential. The units and grid parameters used are the same as in Table VI.

E	$\delta_0^{(0)}$	$\delta_0^{(2)}$	$\delta_0^{(4)}$	E	$\delta_0^{(0)}$	$\delta_0^{(2)}$	$\delta_0^{(4)}$	E	$\delta_0^{(0)}$	$\delta_0^{(2)}$	$\delta_0^{(4)}$
-1.30961	359.7	359.8	359.8	-0.8	304.3	313.5	314.6	0.95	266.8	276.1	277.2
-1.308	355.9	356.8	356.9	-0.55	295.0	304.6	305.7	1.2	264.0	273.1	274.2
-1.3	350.2	352.1	352.4	-0.3	287.7	297.5	298.7	1.45	261.4	270.5	271.5
-1.25	336.8	341.4	341.9	-0.05	282.0	292.0	293.2	1.7	259.1	268.1	269.1
-1.2	329.7	335.7	336.4	0.2	277.5	287.3	288.4	1.95	257.0	265.9	266.9
-1.10	320.5	328.1	329.0	0.45	273.5	283.1	284.2	2.2	255.0	263.9	265.0
-1.05	317.1	325.1	326.1	0.7	270.0	279.4	280.5	2.45	253.5	262.2	263.2

TABLE IX. The parameters for the ${}^4\text{He}-{}^4\text{He}$ Aziz and co-workers potentials used.

Parameter	HFDHE2 [6]	HFD-B [7]	LM2M2 [8]
ε (K)	10.8	10.948	10.97
r_m (Å)	2.9673	2.963	2.9695
A	544850.4	184431.01	189635.353
α	13.353384	10.43329537	10.70203539
β	0	-2.27965105	-1.90740649
C_6	1.3732412	1.36745214	1.34687065
C_8	0.4253785	0.42123807	0.41308398
C_{10}	0.178100	0.17473318	0.17060159
D	1.241314	1.4826	1.4088
A_a	-	-	0.0026
ζ_1	-	-	1.003535949
ζ_2	-	-	1.454790369

TABLE X. The parameters for the ${}^4\text{He}-{}^4\text{He}$ TTY potential used.

A (K)	315766.2067 ^{a)}	C_6	1.461
β ((a.u.) ⁻¹)	1.3443	C_8	14.11
D	7.449	C_{10}	183.5
N	12		

^{a)}The value of A was obtained from the data presented in [9] using, for converting the energy units, the factor $1 \text{ K} = 3.1669 \times 10^{-6} \text{ a.u.}$

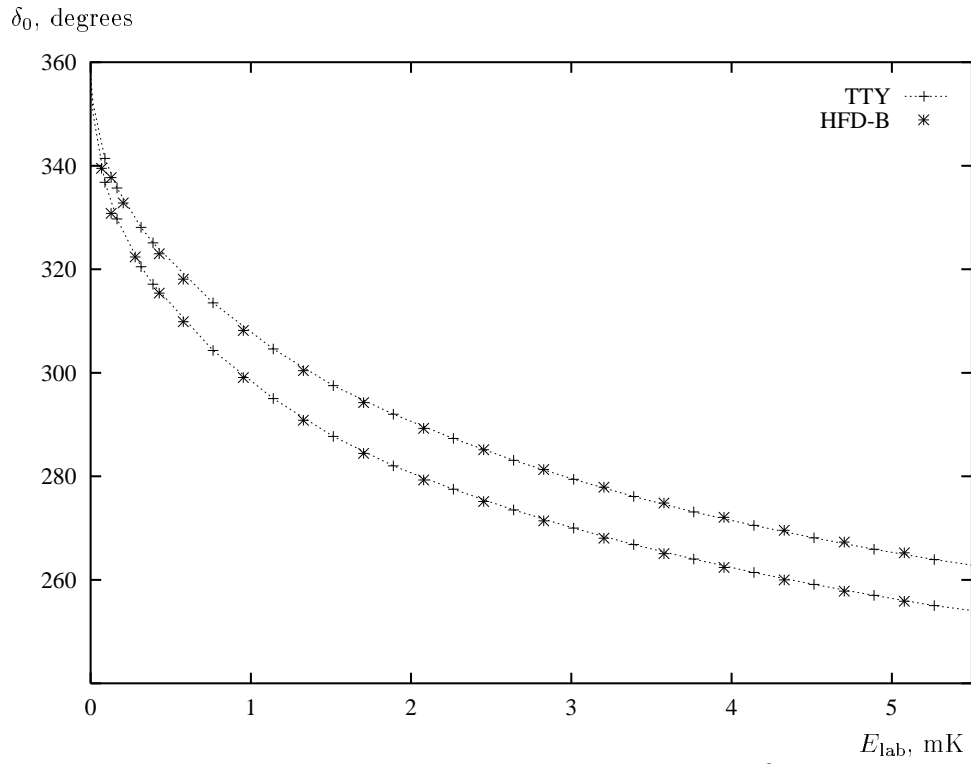


FIG. 1. S-wave helium atom – helium dimer scattering phase shifts $\delta_0(E_{\text{lab}})$, $E_{\text{lab}} = \frac{3}{2}(E + |\epsilon_d|)$, for the HFD-B and TTY ${}^4\text{He}-{}^4\text{He}$ potentials. The lower curve corresponds to the case where $l_{\text{max}} = 0$ while for the upper $l_{\text{max}} = 2$.